

# Reversed Flow through a Kaplan Runner

An investigation of the flow characteristics of a Kaplan runner operating as a pump under reversed-flow conditions

By DR. R. N. KAR

## PART TWO

### Two-Dimensional Cascade of Aerofoils under Normal and Reversed Flow

Next a stationary two-dimensional cascade of representative profiles (Gö 428) was theoretically investigated for determining the cascade influence coefficients under various arrangements—normal turbine, normal pump, and turbine as a pump cascade. These results have been used for comparison with experimental data.

The Schlichting method<sup>5</sup> was applied for these investigations and the complete calculations are given in Ref. 6. The choice of this method was primarily made in so far as it clearly differentiates between the handling of a turbine cascade and a pump cascade, unlike many other methods, such as Betz<sup>8</sup> or Weinig<sup>9</sup>.

### Turbine Cascade Lift (Normal Turbine Case TT)

With the method mentioned under the preceding heading, the turbine cascade lift coefficients for blade angles  $\beta_s = 15, 22.5, 30$  and  $45^\circ$  were calculated for profile Gö 428 with  $t/l$  (pitch-chord ratio) = 1.25 and 1. The calculated values for  $t/l = 1.25$  are given in Fig. 8, where for comparison, the broken line represents the case of a single aerofoil ( $t/l = \infty$ ). From the tabulated results, in Ref. 6 and Fig. 8, one can see that the cascade influence coefficient  $K_{AB} = \zeta_{AB}/\zeta_A = f(t/l, \beta_s, \alpha)$  is very slightly affected by the angle of attack  $\alpha$ ; consequently for all practical purposes one can make it dependent only on vane angle  $\beta_s$  and pitch-chord

ratio  $t/l$ . From Fig. 9 one can see that the theoretical values obtained above by Schlichting's method and the values given by Weinig<sup>9</sup> and those obtained experimentally on a rotating turbine cascade by Hahn<sup>10</sup> differ at the most by 10%.

### Pump Cascade Lift (Normal Pump PP)

In a similar manner, the pump cascade lift coefficients  $\zeta_{AV}$  were calculated and are shown in Fig. 10 for  $t/l = 1.25$ . Again the cascade influence coefficient  $K_{AV} = \zeta_{AV}/\zeta_A$  can be regarded as independent of  $\alpha$ , and is represented in Fig. 11. One can see from this figure that the theoretical values according to Weinig<sup>9</sup> and Weinel<sup>11</sup> deviate by about 15% from the experimental values obtained on a rotating pump cascade given in Table II. On the other hand the theoretical values according to Schlichting's method<sup>5</sup> show a closer agreement.

### Cascade Lift under Reversed Flow (Turbine as a Pump Case TP)

Since under reversed-flow conditions separation takes place near the thick rounded-off trailing edge (normally leading edge) any assessment of cascade lift by a potential-flow theory in this case would not lead to a satisfactory solution. Nevertheless in this case too, by application of Schlichting's method it has been shown in Ref. 6 that for all values of  $t/l$  and vane angle  $\beta'_s$ , the cascade influence coefficient  $K'_{AV} = \zeta'_{AV}/$

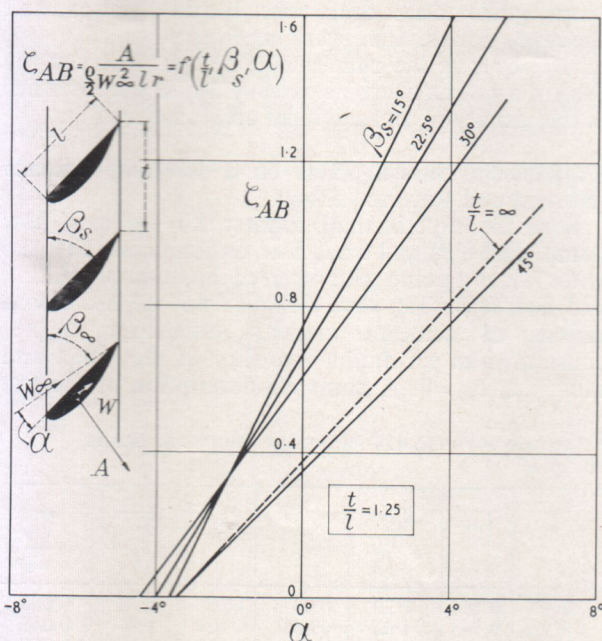


Fig. 8

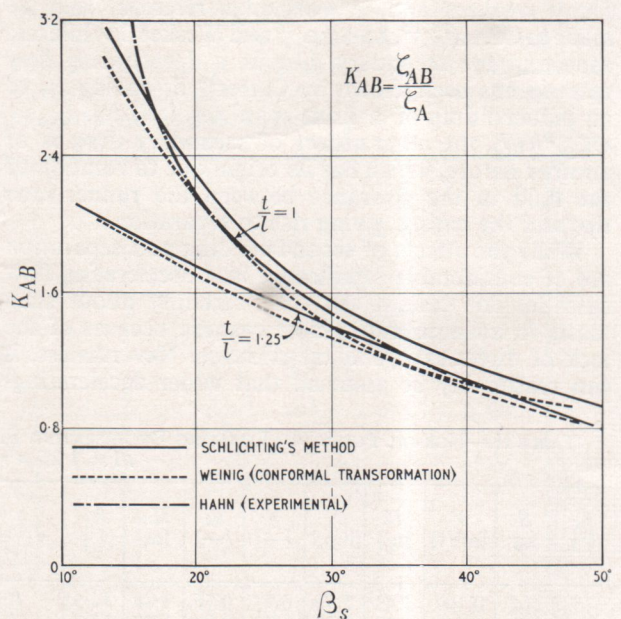


Fig. 9

$\zeta'_A$  for the case TP (turbine as a pump) is less than that for a turbine cascade (TT), i.e.,  $K'_{AV} < K_{AB}$ . This leads exactly to a similar finding as given by the comparison of Figs. 9 and 11.

### Drag in a Turbine and a Pump Cascade

As will be seen later, the experimental values of three-dimensional rotating cascade drag for a decelerating flow (pump cascade) are considerably higher than the individual aerofoil drag. If we take into consideration only the two-dimensional drag in a decelerating cascade as given by Scholz and Speidel<sup>12</sup> or Shimoyama<sup>13</sup>, a significant proportion is still left (compared with three-dimensional drag) which should be attributed to the effects of secondary drag. The phenomenon of second-

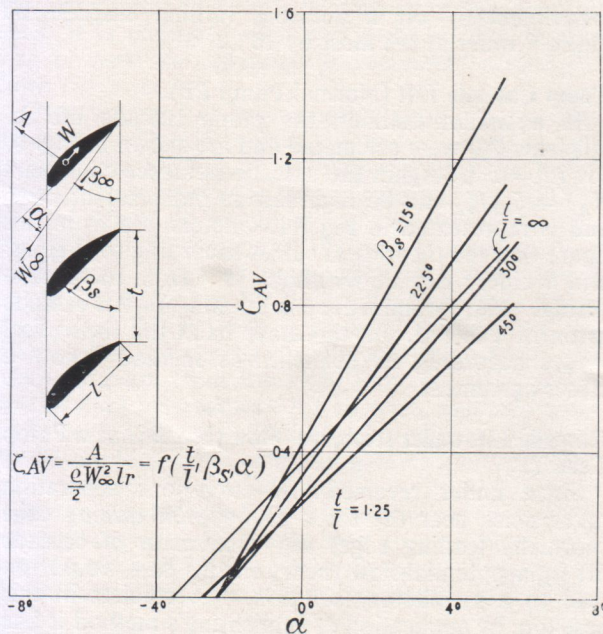


Fig. 10

ary cascade drag has been investigated in detail by many workers<sup>14,15</sup> and in particular reference can be made to Carter<sup>14,15</sup>, Meldha<sup>16</sup> and Weske<sup>17</sup>. While one aspect of the secondary drag in a decelerating flow cascade has been shown by Carter<sup>14</sup> as analogous to an induced drag of a finite-span aerofoil, i.e.  $\zeta_{ws} = C \zeta_{AV}^2 / (t/l)$ , the other aspect of secondary drag is of another nature, which has its origin due to rotation of the fluid in the clearance between the runner-vane tips and the casing, giving rise to separation.

While the effects of secondary drag and separation are of considerable significance in a decelerating-flow cascade, one cannot say with certainty about such losses in an accelerating-flow cascade because of the lack of direct experimental evidence. Nevertheless, it can reasonably be assumed that under accelerating-

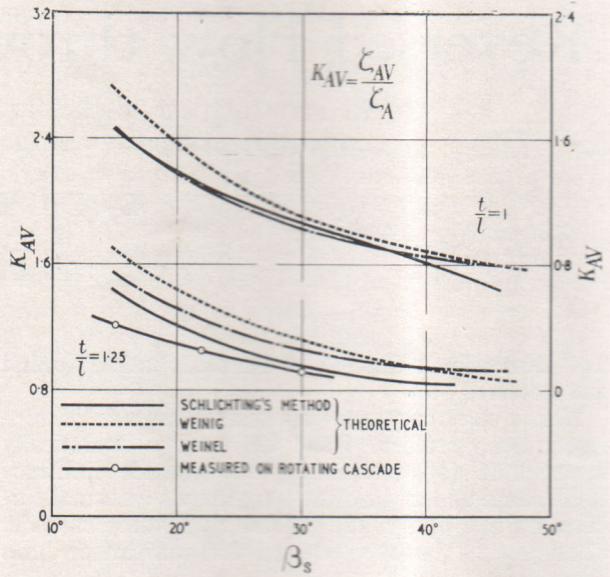


Fig. 11

flow conditions in a turbine cascade, the effects of secondary drag are very small due to the presence of relatively thinner boundary layer. Also in a rotating turbine cascade it can be imagined that the boundary layer built up by centrifugal force near the blade tips is sucked away, since it lies on the suction side, in the direction of flow. Thereby the adverse effects of the centrifugal force and Coriolis component, which have been well established in the case of rotating decelerating-flow cascades by Himmelskamp<sup>18</sup> and Muesmann<sup>19</sup> disappear to a great extent in the case of an accelerating-flow turbine cascade. The effect of pressure drop in the case of an accelerating-flow cascade can even result in a decrease of cascade drag against that of a single aerofoil as is described in the theoretical investigations of Vasandani<sup>20</sup> and Scholz and Speidel<sup>12</sup>. These assumptions are further supported by the practical consideration that a turbine can achieve over 90% efficiency. If one takes into account all the losses due to spiral, guide vanes, draft tube, bearing friction, and clearance losses, then very seldom more than 2% losses occur in the runner-vane system. Thereby the drag in a rotating turbine cascade for all purposes lies in the vicinity of an individual aerofoil drag.

### Experimental Investigations on a Rotating Cascade (Normal and Reversed Flow)

Both the experimental runners for the axial-flow pump (case PP) and axial-flow turbine (case TT), the latter run as a pump with reversed direction of rotation and flow (case TP) were designed for the usual conditions of constant angular momentum ( $c_{u3}r = \text{constant}$ ) and a rotation free flow at the outlet and inlet, i.e.,  $c_{u0} = 0$ . A complete description of the test

TABLE II.—NORMAL PUMP (PP) ROTATING DECELERATING FLOW CASCADE WITH GÖ 428 PROFILE IN MIDDLE OF BLADE,  $t/l = 1.25$ ,  $n = 790$  r.p.m.

$\beta_s$ [°]	S kg	V [m <sup>3</sup> /s]	H [m]	N [h.p.]	$\eta$ [—]	$\eta_b$ [—]	H <sub>th</sub> [m]	$\beta_{\infty}$ [°]	$\alpha = \beta_s - \beta_{\infty}$ [°]	$\zeta_A$	$\zeta_{AV}$	$\frac{K_{AV}}{\zeta_{AV}} = \frac{\zeta_{AV}}{\zeta_A}$	$\zeta_W$	$\zeta_{WV}$	$\frac{K_{WV}}{\zeta_{WV}} = \frac{\zeta_{WV}}{\zeta_W}$	$\frac{\epsilon_V}{\zeta_{WV}} = \frac{\zeta_{WV}}{\zeta_{AV}}$
15	102	0.107	1.43	2.79	0.73	0.76	1.88	14.5	0.5	0.47	0.564	1.20	0.0075	0.02	2.72	0.038
22	108	0.158	1.53	4.19	0.77	0.80	1.91	20.7	1.3	0.535	0.565	1.06	0.008	0.024	2.94	0.042
30	114	0.226	1.66	6.34	0.79	0.82	2.02	27.9	2.1	0.62	0.567	0.92	0.009	0.025	2.81	0.045

TABLE III.—TURBINE RUN AS A PUMP (TP) ROTATING DECELERATING FLOW CASCADE WITH GÖ 428 PROFILE IN MIDDLE OF BLADE,  $t/l = 1.25$ ,  $n = 770$  r.p.m.

$\beta'_s$ [°]	$S'$ kg	$V'$ [m <sup>3</sup> /s]	$H'$ [m]	$N'$ [h.p.]	$\eta'$ [—]	$\eta'_h$ [—]	$H'_{th}$ [m]	$\beta'^\infty$ [°]	$\alpha' = \beta'_s - \beta'^\infty$ [°]	$\zeta'_A$	$\zeta'_{AV}$	$K'_{AV} = \frac{\zeta'_{AV}}{\zeta'_A}$	$\zeta'_w$	$\zeta'_{wv}$	$K'_{wv} = \frac{\zeta'_{wv}}{\zeta'_w}$	$\epsilon'_v = \frac{\zeta'_{wv}}{\zeta'_{AV}}$
15	69	0.098	0.99	2.1	0.61	0.64	1.54	14.2	0.8	0.34	0.37	1.09	0.014	0.049	3.42	0.133
22	70	0.151	0.96	3.1	0.63	0.66	1.46	20.5	1.5	0.40	0.36	0.9	0.014	0.050	3.57	0.138
30	80	0.225	1.14	5.23	0.65	0.68	1.67	27.5	2.5	0.50	0.40	0.8	0.016	0.056	3.5	0.14

stand is given in Ref. 6. The runner had a diameter of 300 mm and the blade profile in the middle was Gö 428 with corresponding  $t/l = 1.25$ . The main purpose of these experiments, which were carried out at the Indian Institute of Technology (Kharapur, India) was to determine for a normal pump (PP) and turbine as a pump (TP) the cascade lift and drag coefficients. To achieve this the axial thrust, torque, speed, head and quantity of flow were measured. The measurement of axial thrust by a sensitive propeller dynamometer

efficients, is a noteworthy departure. The procedure for arriving at the cascade aerodynamic coefficients is described in detail in Ref. 6, and here only the end results in Tables II and III and the characteristic diagrams Figs. 12, 13 and 14 have been reproduced. As has been mentioned before, no experimental cascade results for a normal turbine (TT) have been investigated, as these are important only for comparison with the case when it is run as a pump (TP). However, theoretical turbine cascade results have been adopted from preceding sections for purposes of comparison.

### Results of Measurement on Normal Pump Operation (Case PP, Fig. 1a)

For normal pump operation the points of best efficiency for different vane angles as derived from the experimental data in Table II are plotted in Fig. 13. The experimentally evaluated values for cascade lift influence coefficients  $K_{AV}$ , in Table II are reproduced in Figs. 11 and 15. The theoretical values of  $K_{AV}$  according to Schlichting's method are in better agreement with the experimental values than those by Weinel and Weinig. Further, the experimental values of cascade drag in Table II and Fig. 18 show that it can be as much as three times the single aerofoil drag  $\zeta_w$ . The treatment of a two-dimensional pump cascade by Scholz and Speidel<sup>12</sup> and Shimoyama<sup>13</sup> does of course show a considerable increase in cascade drag compared with a single aerofoil, but in a rotating cascade as above this increase is further enhanced by secondary drag. Thereby only two-dimensional cascade drag can be regarded as unsatisfactory. These observations do qualitatively indicate an agreement with the results of the work by Carter and Cohen<sup>15</sup> and also Howell<sup>21</sup>, in which the authors point out that the secondary drag can contribute a very significant part towards the total cascade drag.

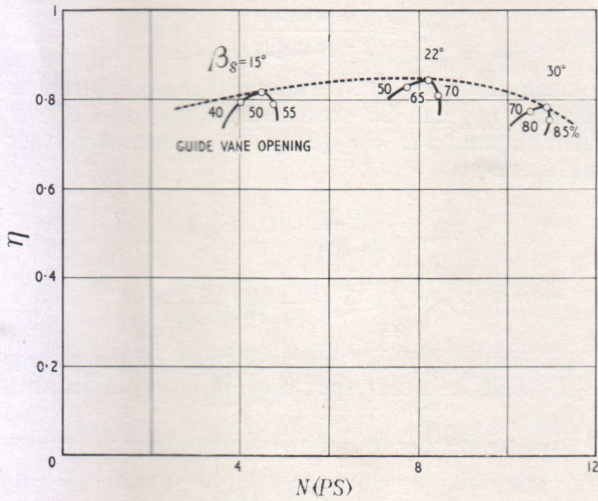


Fig. 12

instead of the usual complicated pressure and velocity distributions near the runner inlet and outlet or pressure measurements on a rotating runner-vane surface, needed for arriving at the cascade aerodynamic co-

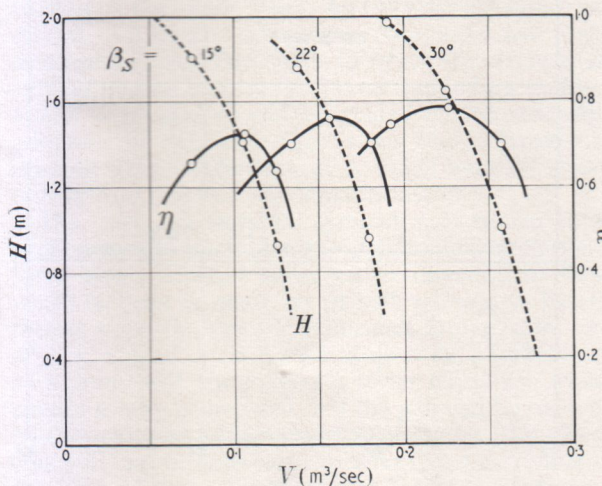


Fig. 13

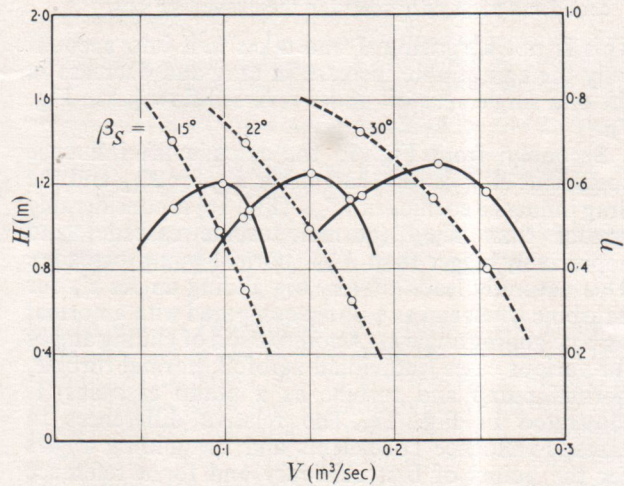


Fig. 14

**Results of Measurement on a Turbine Cascade when Run as a Pump (Case TP, Fig. 1d)**

When a turbine is run as a pump (case TP), the rotating cascade represents a decelerating flow. The measured and evaluated efficiency cascade influence

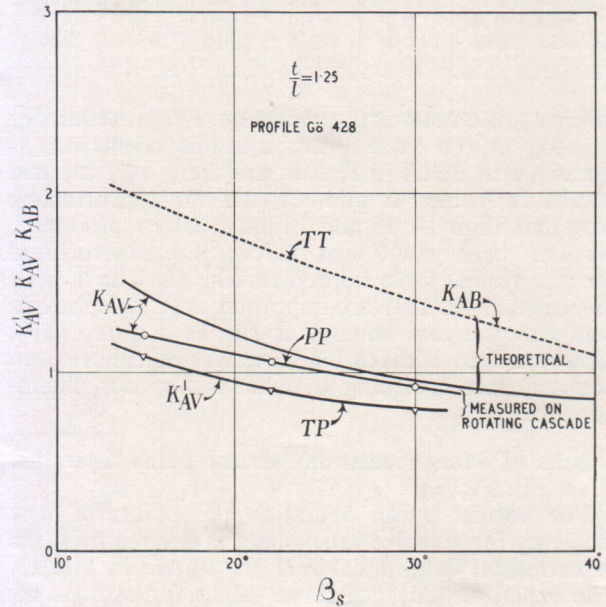


Fig. 15

coefficients for lift and drag in Table III have been reproduced in Figs. 14, 15 and 16 respectively. The values for individual aerofoil lift and drag coefficients have been taken from the experimental results in Fig. 7. Qualitatively the same trend in the cascade drag, i.e., a considerable increase over the individual aerofoil drag, is also present in this case as in the case PP (normal pump).

**Conclusions**

Figs. 12, 13 and 14 show a maximum efficiency of 83%, 78% and 65% for a normal turbine, a normal pump and for a turbine run as a pump respectively.\*

\* These values pertain to the model tested and can quantitatively vary with other models. Nevertheless for a conventional turbine-blade design the efficiency as a pump will always be considerably less as indicated in these investigations.

This is not surprising if one takes first into account only the appreciable increase in drag and decrease in lift of a single aerofoil under reversed flow (as in Fig. 7).

Secondly, from Fig. 15 the cascade lift influence coefficient  $K'_{AV}$  is less than either  $K_{AV}$  or  $K_{AB}$  and the drag influence coefficient  $K'_{WV}$  (Fig. 16) is considerably greater than  $K_{WB}$  (normal turbine cascade) and appreciably bigger than  $K_{WV}$  (normal pump cascade). This naturally leads to very big gliding angles  $\epsilon'_V$  for a turbine when run as a pump compared with a normal turbine gliding angle  $\epsilon_B$ . A comparison of gliding angles for various cases (individual aerofoil, normal turbine, normal pump and turbine as a pump cascades) is illustrated in Fig. 17. The relative differences in cascade influence coefficients and the gliding angles for the points of best efficiency and for a reference cascade profile section in the middle of the runner blade are given in Table IV.

TABLE IV

Accelerating Flow Cascade Normal Turbine (TT)	Decelerating Flow Cascade Normal Pump (PP)	Taken from
$K'_{AV}/K_{AB} \approx 0.6$	$K'_{AV}/K_{AV} \approx 0.9$	Fig. 15
$K_{WV}/K_{WB} \approx 3.5$	$K_{WV}/K_{WV} \approx 1.2$	Fig. 16
$\epsilon'_V/\epsilon_B \approx 9$	$\epsilon'_V/\epsilon_V \approx 3.5$	Fig. 17

It should of course be noted here that for comparison above only the theoretical values for a turbine cascade (TT) have been taken against the measured ones for cases PP and TP.

The operation of a turbine as a pump gives rise to the distinct disadvantage of having a great increase in the gliding angle. This is directly responsible for a substantial decrease in the efficiency, as can be seen from the following efficiency equation of Betz<sup>23</sup> for a decelerating flow cascade:

$$\eta_V = \frac{1 + |\epsilon \tan \beta_\infty|}{1 - |\epsilon \cot \beta_\infty|}$$

Again according to Muesmann<sup>19</sup>, the pump-runner efficiency  $\eta_{VL}$  can be expressed on the basis of the Euleren equation  $H = \eta_{VL} \Delta C_u r \omega / g$  which when further transformed is

$$\eta_{VL} = \frac{Hg}{\Delta C_u r \omega} = 1 - (1 - \eta_V) \left| \frac{W_{u\infty}}{r\omega} \right|$$

This clearly explains that an increase in the gliding angle results in a corresponding efficiency reduction.

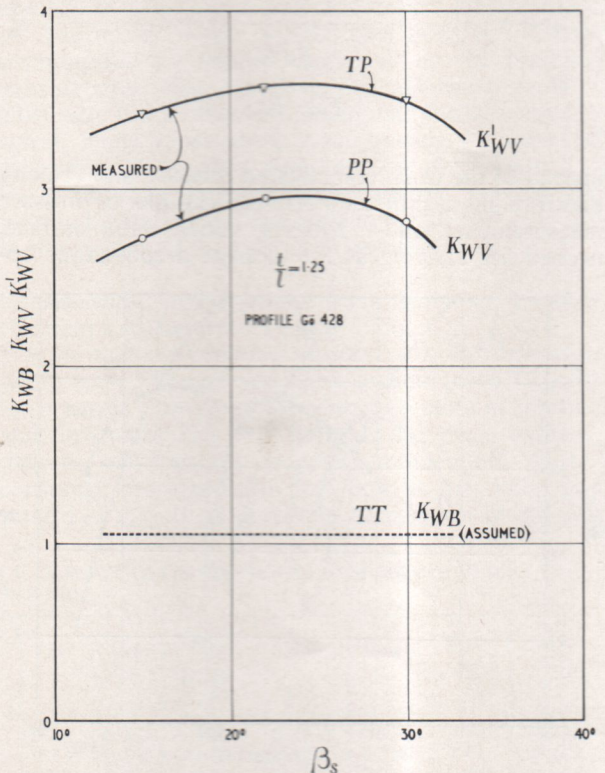


Fig. 16

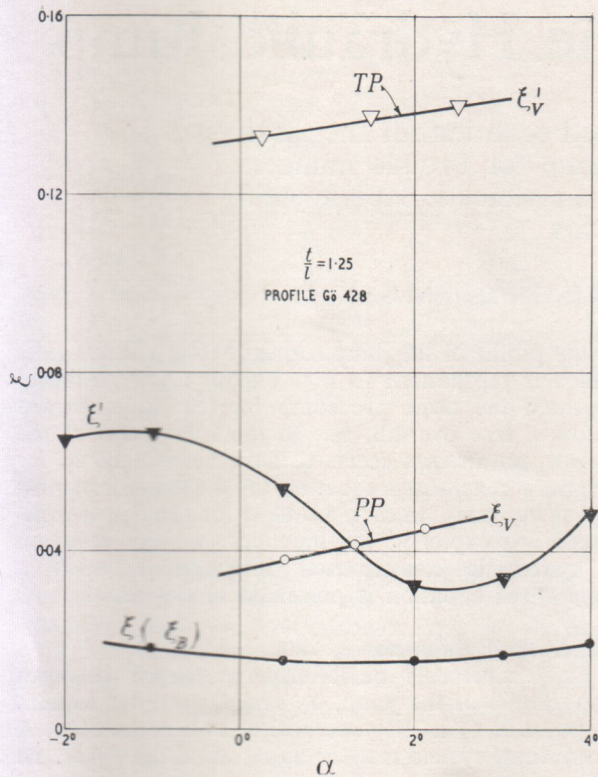


Fig. 17

However, in the light of above investigations the difference in efficiency between cases TT and TP could be reduced by adopting the following suggestions:

- (i) The runner-vane profiles at and near the hub should be thinner or have less camber.
- (ii) Symmetrical profiles for the runner vanes may be used.
- (iii) Guide-vane profiles near the root may have less camber or thickness. One could in general use symmetrical profiles for guide vanes, which should not appreciably affect the turbine efficiency.

One can only recommend the adoption of suggestion (i) with reservations. In order to achieve the desired lift from a less-cambered section bigger angles of attack are necessary near the hub sections, which would result in a turbine-blade form of a smaller twist. On the other hand, under reversed-flow conditions as a pump such a procedure could still prove disadvantageous. The extent to which the decrease in camber and an increase in the corresponding angle of attack is affected should be guided by the minimum adoption of  $\Delta\zeta_A$  and  $\Delta\zeta_W$  values (the difference in lift and drag coefficients of a single aerofoil under normal and reversed-flow conditions).

The use of suitable symmetrical runner-blade profiles results in similar aerodynamic characteristics for a single aerofoil under either direction of flow, which fact can be made use of with advantage. Nevertheless since the cascade influences are adverse, i.e.,  $K'_{AV} < K_{AB}$ ,  $K'_{WV} > K_{WB}$  and  $e'_V > e_B$ , a turbine run as a pump will always give a lower efficiency, which cannot totally be avoided, but the gap can be reduced by the adoption of the above suggestions. The use of conventional turbine-blade profiles is not advisable in the light of these investigations if it is to work as a pump.

Lastly, as regards cavitation, both the experimental and theoretical investigations on a single aerofoil show that for small positive angles of attack under reversed flow, the low-pressure peaks are not greater than those under normal conditions of flow, which would lead to an assumption of no increase in cavitation. However, the actual cavitation behaviour can be studied by proper model tests.

REFERENCES

1. BROWN, C. E., "The Reversibility Theorem for Thin Airfoils in Subsonic and Supersonic Flow," NACA Report 986, 1950.
2. Ergebnisse der Aerodynamischen Versuchsanstalt Göttingen, I. und II. Lieferung, München-Berlin, 1921.
3. LOCK, C. N. H. and TOWNEND, H. C. H., "Lift and Drag Aerofoils Measured over 360° Range of Incidence," A.R.C.R. and M., No. 958, Nov. 1924.
4. POP, ALAN, "Summary Report of the Forces and Moments over a NACA 0015 Airfoil, Through 180° of Attack," *Aero Digest*, Apr. 1949.
5. SCHLICHTING, H. "Berechnung der reibungslosen inkompressiblen Strömung für ein vorgegebenes ebenes Schaufelgitter," *VDI-Forschungsheft* 447, Ausg. B, Bd. 21, 1955.
6. KAR, R. N., Allgemeine Betrachtungen über die Umkehrung der Strömungsrichtung eines Kaplanrades (Vollständige Fassung), Diss. TH München, 1959.
7. BETZ, A., "Mechanik unelastischer Flüssigkeiten," Hütte I, 28, Aufl 1955, S. 807.
8. BETZ, A., "Konforme Abbildung," Berlin-Göttingen-Heidelberg, 1948.
9. WEINIG, F., "Die Strömung um die Schaufeln von Turbomaschinen," Leipzig, 1935.
10. HAHN, K., Untersuchung der Strömung durch eine Flügelradturbine bei verschiedenen Schaufelzahlen, Diss. TH Karlsruhe, 1933.
11. WEINEL, E., "Beitrag zur rationellen Hydrodynamik der Gitterströmung," *Ing. Arch.* 5, 1934.
12. SCHOLZ and SPEIDEL, "Untersuchungen über die Strömungsverluste in ebenen Schaufelgittern," *VDI-Forschungsheft* 464, Apr. 1957.
13. SHIMOYAMA, "Experiments on Rows of Aerofoils for Retarded Flow," *Kyushu Imp. Un.*, Vol. VIII, 1938.
14. CARTER, A. D. S., "Three-dimensional Flow Theories for Axial Compressors and Turbines," *Proc. I. Mech. E.*, Vol. 159, 1948.
15. COHEN, M. and CARTER, A. D. S., "Preliminary Investigation into the Three-dimensional Flow Through a Cascade of Aerofoils," A.R.C. Technical Report, R. and M., No. 2339, H.M.S. Office, London, 1949.
16. MELDAHL, A., "The End Losses of Turbine Blades," *Brown-Boveri Review*, Vol. 28, 1941.
17. WESKE, J. R., "Fluid Dynamics Aspects of Axial-Flow Compressors and Turbines," *J. Aeron. Sc.*, Vol. 14, 1947.
18. HIMMELSKAMP, H., "Profiluntersuchungen an einem umlaufenden Propeller." Mitteilung 2 aus dem Max-Planck-Institut für Strömungsforschung, Göttingen, 1950.
19. MUESMANN, G., "Zusammenhang der Strömungseigenschaften des Laufrades eines Axialgebläses mit denen eines Einzelflügels," *Z. Flugwiss.* 6, 195, S. 345/62.
20. VASANDANI, V. P., Theoretische Untersuchung des Gittereinflusses auf Auftrieb und Widerstand in zweidimensional durchströmten Turbinen und Pumpengittern. Diss. München, 1959.
21. HOWELL, A. R., "The Aerodynamics of the Gas Turbine," *J. Roy. Aero. Soc.*, Vol. 52, 1948.
22. BETZ, A., "Tragflügel und hydraulische Maschinen in Geiger-Scheel," *Handbuch der Physik*, Bd. 7, S. 256, Berlin, 1927.
23. BETZ, A., "Einführung in die Theorie der Strömungsmaschinen," Karlsruhe, 1959.

**Geotechnical Pamphlets.** Soil Mechanics Limited have sent us the last two issues in their series of Geotechnical Pamphlets. No. 12 is a reprint of an article on corrosion and site investigation which first appeared in the September 1961 issue of *Corrosion Technology*. The second pamphlet, No 13, describes the laboratory testing facilities of Soil Mechanics Limited.